DOI: 10.53469/jpce.2025.07(11).05

Observation Study of Stratiform Precipitation and Cloud Microphysical Structures During a Flight Detection Over Liupan Mountain Areas

Lei Tian[1], Zhuolin Chang[2,] *, Haoran Zhu[3], Tong lin[4], Ning Cao[5], Yanqiao Sun[6]

[1,2,3,4,5,6]Key Laboratory for Meteorological Disaster Monitoring and Early Warning and Risk Management of Characteristic Agriculture in Arid Regions, CMA, Yinchuan 750002, China
[1,2,3,4,5,6]Ningxia Meteorological Disaster Prevention Technology Center, Yinchuan 750002, China
[1]tianl419@126.com, [2]changzhl05@126. com, [3]kevin_zjhz@126.com, [4]lintong0213@126.com, [5]caoning_2007@163.com, [6]yanqiaosun@126.com
**Correspondence Author*

Abstract: ***A flight detection with stratiform precipitation on September 19th, 2018 is chosen for analysis. Through the level flight, circling and repeated detection after seeding, the cloud structures of Liupan mountain is profiled. The microphysical structures of stratiform clouds, the precipitation enhancement conditions as well as physical responses after cloud seeding are studied. The results show that the thickness of mixed clouds are larger than 5km, interlayer is found in mixed clouds, the 0°C temperature layer is at a height range of 4800-5000 m. There are significant differences between the macro and micro physical structures at East and West side of Liupan mountains and surface precipitation can be seen in both sides. At West side of Liupan Mountain, the clouds which contain three layers are thicker, the upper two layers are mainly formed by ice particles, the spectrum of particle size is wide, the number concentration is comparatively small, precipitation is mainly from bottom layer of mixed clouds, the supercooled water lead to enhanced condensation growth. At East side of Liupan Mountain, there is no interlayer, the increase of cloud particles is milder than West side. Supercooled water exist in the top and middle part of stratiform cloud, which is suitable for cold cloud seeding operations.***

Keywords: Aircraft observation, Cloud microphysical structure, Supercooled water, Liupan Mountain, Particle spectrum.

1. Introduction

The cloud plays an essential role in weather and climate systems. For one thing, The structures, physical features and constitute of hydrometeor place significant influence on evolution of weather processes. For another, different types of clouds show different feedback effects corresponding to atmospheric radiation processes, which can further affect global energy budgets (Fu et al., 2007). The microphysical structures of clouds are of importance in cloud and precipitation research, of which the aircraft field observation is a key method to obtain micro and macro physical parameters of clouds (Ma et al., 2012).

In 1970s, PMS is used in detection of different cloud systems. The raindrop size distribution in Frontal cloud system of extratropical cyclone is obtained through systematic field observations (Houze et al., 1979). In fact, there exists supercooled water layer on top of most stratiform and cumulus clouds and the seeding-feeding mechanisms are obvious in the formation of stratiform clouds (Hobbs et al., 1980; 1985). In 1980s, PMS is applied for stratiform cloud observations in China. There are a variety of findings. Yang et al. (2005) found that stratiform cloud precipitation systems are inhomogeneous and the cloud water content peaks at the lower part of the cloud inversion layer through the analysis of PMS observation in Hebei in springtime. Hong et al. (2011), Hou et al. (2011) found that "seeding-feeding" is the the main mechanism in Cold front precipitation through flight detection and numerical simulations. The vertical structures show difference in different parts of clouds in which there are ice cloud layer, ice-water mixed layer and liquid water layer from top to bottom. The moisture content center of these three areas are at 300hPa, 600-650hPa and 800-900hPa pressure level. Zhang et al. (2011) found that the cloud particle' content is proportional to it's diameter in fore of cold front cloud system using PMS data of microphysical structure features retrieved by airplane in the vicinity of Beijing. Cloud particle size distribution is unimodal at 4800m, multi-modal at 4200m, and bimodal at 3600m. Zhang et al. (2012) analyzed the cloud microphysical structure features in Hebei province using the PMS data. It is found the number of cloud drop in cloud bottom is larger than that in top and middle of cloud and the drop size increases by height. Specifically, the largest liquid water content in cloud is 0.25g•m^{-3}, the mean liquid water content in cloud bottom is 0.025g•m^{-3}, the number concentration in middle and upper layer of mixed cloud is larger than that in bottom layer. The cloud number concentration varies from 10 to 80 cm^{-3}. Besides, the mean cloud drop diameter is 7.56μm which increases first and then decreases with the ascent of altitude. The microphysical features and weather modification conditions are comprehensively analyzed by Sun et al. (2015) and Qin et al. (2015, 2017) using PMS data. What's more, the microphysical features of stratiform cloud in Gansu located in the Northwestern China is analyzed through PMS data by Dang et al. (2009), Pang et al. (2016) and Wang et al. (2017). In order to analyze the microphysical features of multi-layer stratiform cloud closely in Jiangyuan Area. To achieve this purpose, the concentrations of liquid and ice cloud particles, the evolution of cloud drop spectrum and supercooled water content ratio before operations are compared with those after operations. In Ningxia, the micro and macro physical features of stratiform cloud are studied by Xiang et al. (2008) and Fan et al. (2000) using PMS data. It is found that there are multiple crest values throughout the vertical distributions of stratiform cloud water content and the largest value occurs in the middle and bottom layer of cloud.

For recent decades, DMT method is broadly applied in cloud physics studies. Ma et al. (2012) looked into the flight detection of the rear of subtropical high stratiform cloud in August 18th, 2010. The results showed that the cold clouds exist in upper layer while the warm clouds exist in bottom layer; the vertical distribution of liquid water content in warm clouds are bimodal, the Frontal zone exists in the top and bottom of warm stratiform cloud and the peak value is around 0.8~1.0g/m³; The crest value area of solid water concentration exist in cloud water area and the peaak values of ice concentration and snow concentration are 250~350L^{-1} and 12~16L^{-1}, respectively. Huang et al. (2005) summmarized that the cloud drop concentration and water content of stratiform cloud in Huabei in springtime are 10~200cm^{-3} and 0.01 0.1g•m^{-3}, respectively. Besides, the fluctuation of cloud drop concentration in spring is larger than that in autumn. Feng et al. (2014) studied macro and microphysical features of stratiform cold cloud in Shanxi and revealed that precipitation clouds consist of Stratospheric cloud and Stratocumulus where the liquid water content varies from 0 to 0.42g•m^{-3}; in addition, it is high the cloud drop spectrum show an unimodal or bimodal pattern; the exponential type pattern usually appear at the middle and top of Stratocumulus. Qi et al. (2019) analyzed the structure features of Stratus-cumulus mixing clouds during a precipitation in May 22th, 2017 at the east slop of Taihang Mountain; it is found that the convective bubble dotted in stratiform cloud usually exist at −10~0℃ temperature layers (which correspond to 4-6km height layers), the vertical and horizontal scale are 2km, the maximum updraft velocity is 5m•s^{-1}.The mean liquid water content in convective bubble is as twice as that in surrounding areas, the mean small cloud particle is ten times larger that in surrounding areas. Sun et al. (2019) analyzed the microphysical structures and weather modification conditions and found that the supercooled water content can reach up to 0.2g•m^{-3} at 5000m or higher altitude, which is 2~4 times larger than that in stable stratiform cloud; The supercooled layerwith temperature at -15~-5℃ is a key area for ice growth which is suitable for cloud seeding. Through aircraft observation, Chang and Guo et al. (2019) found that the concentration of cumulus droplets (In diameter, between 2~50 μm) in the summer development stage was about 10cm^{-3}, about 1~2 orders of magnitude lower than that of other regions of the mainland and Marine areas, and the concentration of cloud droplets (Diameter is greater than 50 μm) was about $10^{-3}cm^{-3}$, also lower than that of other regions. The cloud drop spectrum is much wider than that in other regions, indicating that cumulus clouds on the plateau are more likely to form precipitation than those in other regions. Zhao et al. (2018, 2019) used the observation data of 6 aircraft sorties in Hebei in September 2015 and found that the negative relationship between aerosol and the effective radius of cloud droplets was stronger when the LWC remained unchanged. In the case of pollution, the cloud droplets are distributed in a small size range, and the aerosol-cloud interaction is around 0.10~0.19. On the microphysical characteristics of the warm cloud in the coastal areas of China on April 26th, 2010. we found that the aerosol concentration of 0.1~3 μm and CCN large area appeared in the planetary boundary layer (PBL) below 1150m. However, the aerosol concentration and CCN decreased rapidly with increasing height. The effective radius of cloud droplets below 1150m is small (3~6 μm), and the effective radius of cloud droplets above PBL is large (7~13 μm). In the PBL clouds, the cloud droplet effective radius was negatively correlated with the aerosol concentration, with a clear positive correlation at the height above the PBL. With increasing LWC values, the relationship between the effective radius of cloud droplets and the aerosol number concentration changed from negative to positive correlation. Wang and Niu et al. (2019) studied the Hebei layered cloud in 2015 through the airborne equipment of the aircraft, and proposed a new algorithm to calculate the contribution of droplets of different sizes to the relative dispersion (ε), and found that the diameter of 1~5.5 μm and 5.5~10 μm had a great influence on ε; with the increase of aerosol concentration, ε increased initially, and then decreased. Li et al. (2019) observed the aerosol and cloud in Shanxi Province and found that the effective diameter of aerosol particles was mostly less than 1 μ m, and the number concentration decreased with the increase of height through six aircraft observations in May 2013. The maximum and mean values of the cloud droplet concentration for warm clouds were 147~311cm^{-3} and 51~157cm^{-3}, respectively. The maximum and mean particle diameter diameters were 13.5~28.9 μm and 5.8~13.1 μm, respectively. The average LWC of warm clouds was 0.05g·m^{-3}. Aerosols and cloud droplet number concentrations were negatively associated in both vertical and horizontal directions. In high aerosol environment, the smaller the cloud droplets, the higher the number concentration; in low aerosol environment, a small number of large cloud droplets appear. When the LWC is unchanged, there is a negative correlation between cloud droplet concentration and particle diameter. The cloud droplet size also increased when the LWC increased. The bimodal log-normal distribution function can well fit the average cloud drop spectrum of warm clouds. Wang et al. (2021) used radar, satellite and raindrops spectrometer to observe the first quantitative evidence in China that the AgI catalyst sown by aircraft produced a significant catalytic effect on supercooled clouds with a cloud ceiling temperature of -15℃. Radar echo occurred 18 minutes after catalysis, followed by a distinct ice crystal catalytic trajectory. The radar echo dropped to the surface 40 min after sowing. The maximum diameter of the raindrops produced by the surface raindrop spectrometer is 2.75 mm, while the maximum diameter of the precipitation process is 1 mm. An enhancement of ground-based precipitation was observed within 100 min after catalysis. Dong et al. (2020) studied the difference between supercooled clouds before and after catalysis through aircraft observation. The results show that the target cloud is supercooled liquid clouds before catalysis. After catalysis, large ice crystal particles appear in the cloud and the particle size spectrum becomes wider, which can grow up the microprecipitation particles by touching the merger process. Through an aircraft observation in Baoding, Hebei province on August 5th, 2018, Wei et al. (2022) found that the diameter of most cloud particles was between 7~10 μm in the cumulus, while in the stratus, the diameter of most cloud particles was not more than 2 μm. The effective radius of cloud droplets was negatively correlated with the aerosol concentration of the planetary boundary layer (PBL) and the upper PBL in the cloud. In the area of high liquid water content above 1500 m, the concentration of cloud droplets does not change much, and the concentration of aerosol number decreased. The high radar reflectivity corresponds to the large FCDP cloud particle concentration and the small aerosol particle concentration; strong updraft in the cumulus increases the peak radius and

number concentration of cloud droplets and widens the cloud droplet spectrum; lower air temperature promotes the condensation growth of particles and produces larger droplets.

The DMT observation system is broadly applied in North China whereas less used in other parts of China. Aircraft observation studies are more in Qinghai ang Gansu Province than other Northwestern areas. Stratiform cloud is the typical cloud in spring and autumn time in North China and thus a major weather modification target (Huang et al., 1999). Stratiform cloud has long duriation and stable structure. Although the mechanism of stratiform cloud precipitation is complex, to know its macro and micro physical structures is of significance for precipitation formation mechanisms. The micro physical structures of cloud and precipitation vary with different areas. Liupan mountain is located in the Northeast of Qinghai Tibet Plateau. It lies in the intersection area of the north and south airflow as well as the edge of Monsoon region. The research in Liupan mountain area might be benefit to reveal the influence of complex topography on precipitation cloud structures, which can improve the weather modification techniques in mountaineous areas.

2. Devices, Data and Methods

2.1 Brief Introduction of Devices and Data

The probe devices used here are particle measuring systems carried by MA-60. The cloud particle detectors include CDP (Cloud Droplet Probe) and BCP (Back-Scatter Cloud Probe), of which the measuring range of CDP is 2~50μm and the minimum resolution is 1μm; those of BCP are 5~75μm and 2μm, respectively; those of CIP (Cloud Imaging Probe) are 25~1550μm and 25μm, respectively; and those of PIP (Precipitation Imaging Probe) are 100~6200μm and 100μm, respectively. However, concerning the malfuction of CDP and the consequent large errors, an alternative BCP detector is used here.

2.2 Methods for Data Process

Parameters such as Particle Number Concentrations (N) between 5 to 50μm are calculated through drop spectrum retrieved by BCP. The calculating method is as follow: The cloud drop spectrum in BCP raw data is transformed into number concentration data (the unit is $cm^{-1}\mu m^{-1}$). The calculating formulas are listed as follow:

$$N = \sum_{i=1}^{k} ni$$

$$ni = Ni/(V \times \Delta r)$$

$$V = c/f$$

$$c = S_{sampling} \times V_{true}/f$$

All of them derive the following formula:

$$ni = Ni \times f^2/(S_{sampling} \times V_{true} \times \Delta r)$$

The ni stands for number concentrations in each size group (unit: $cm^{-1}\mu m^{-1}$), Ni stands for drop numbers in each size group, f stands for sampling frequency, $S_{sampling}$ stands for sampling area, V_{true} stands for aircraft vacuum velocity, Δr stands for radius intervals.

In this flight detection process, the sampling area of BCP, CIP and PIP are 0.25mm^2, 155mm^2 and 1612mm^2, the sampling frequency is 1Hz.

The effective diameter in specific diameter range can be calculated as follow:

$$d_{eff} = 2 \times \frac{\int_{r_{min}}^{r_{max}} r^3 n(r) dr}{\int_{r_{min}}^{r_{max}} r^2 n(r) dr}$$

3. Weather Processes and Airplane Probe

3.1 Synoptic Situation

Under the joint influence of cold air mass and warm and moisture airflow outside the subtropical high, rainfall appear in most districts of Ningxia in Setptember 19th, 2018.Figure 1 shows the synoptic situation on 19th. There are two ridges-one trough, and a low pressure in North Xinjiang. The subtropical high is located in Southeastern Ningxia. On the night of 18th and the morning of 19th, the Middle-South Ningxia is affected by shear line in the lower level and the warm and moisture air in the Northwest of subtropical high, during which the rain band moves from South to North. On the afternoon of 19th, the subtropical high subsides gradually and the 500hPa trough pass above Ningxia. Owing to the poor condition of moisture in lower level as well as the abundance of the middle and high level clouds, weak rainfall appear in South Ningxia. From after midnight, Ningxia is gradually controlled by WNW airflow at the rear of trough, where the wind direction at 700hPa layer turned Northwest, with a higher wind speed and subsiding cloud systems, the rainfall is unlikely to form.

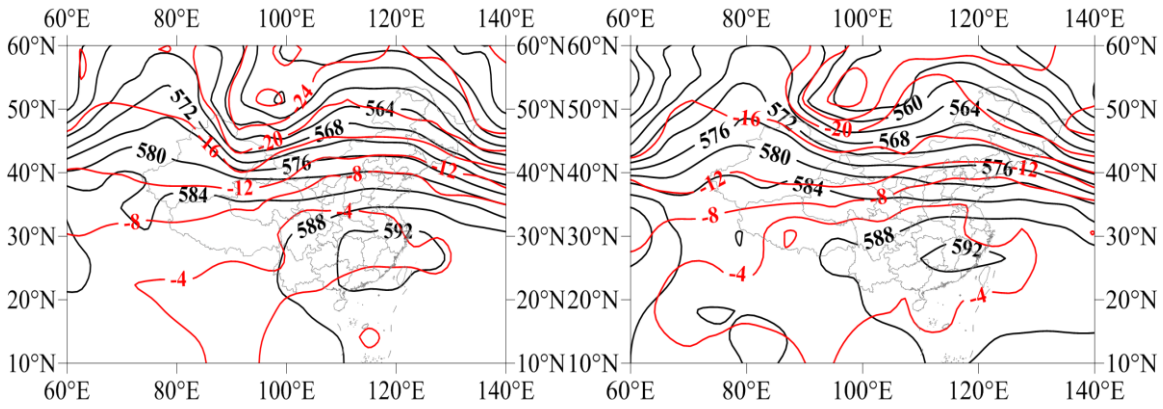

Figure 1: The weather situation field (a: 08: 00 on September 19th, b: 20: 00 on September 19th)

3.2 Overview of Flight Detection

To summarize the features of cloud structures, cloud seeding conditions and cloud microphysical parameters over Liupan Mountain Area, a flight detection is carried out by Meteorological researchers in Ningxia, China. The flight detection is from 06: 00 a.m. to 11: 06 a.m. on 19th, the air route is Yinchuan - Jingyuan - Longde - Jinyuan - Huanxian - Yinchuan. The flight route is shown in Figure 2a and 2b. The flight detection is divided into 3stages.

Stage 3 and 4: Vertical detection at the West fixed point of Liupan Mountain (7: 27-8: 23a.m.); Stage 5 and 6: Level flight over the ridge of Liupan Mountain and toward the East fixed point (8: 24-8: 32a.m.); Stage 7: Vertical detection at the East fixed point of Liupan Mountain (7: 27-8: 23a.m.); Stage 8: Cloud seeding (8: 09: 15-09: 42a.m.); Stage 9 and 10: Cloud seeding repeatedly (09: 43-09: 58a.m.); Stage 11: Detection in return journey (9: 58-10: 54a.m.).

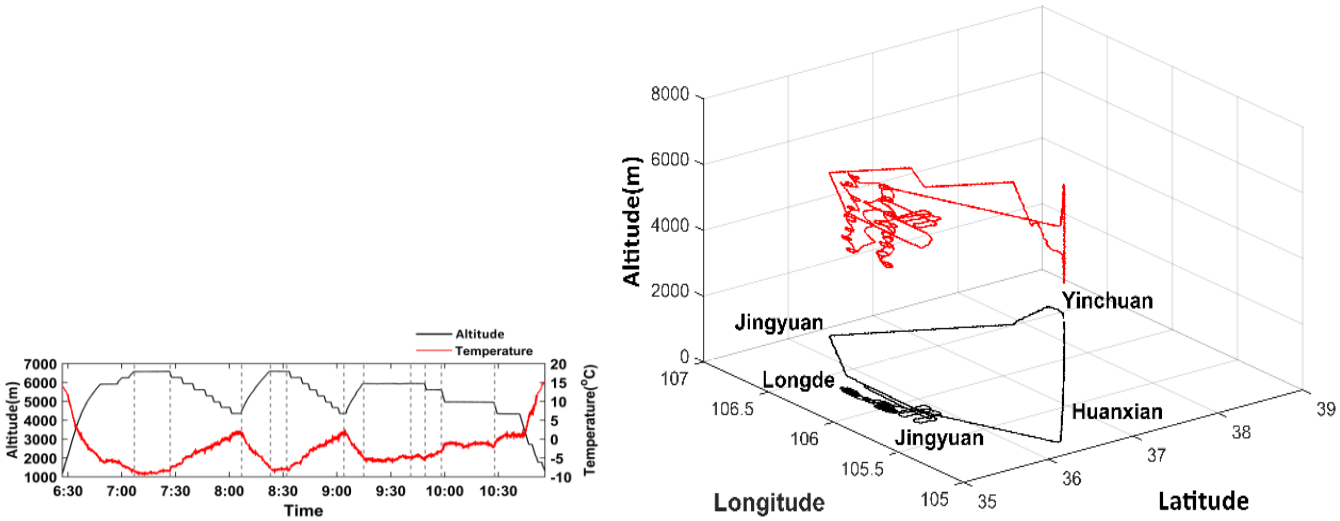

Figure 2: Catalyst track map for aircraft detection on Setptember 19th, 2018 (a: The black line is the flight height, and the dark gray line is the temperature of the flight height. b: The black line and the deep gray line are three-dimensional and two-dimensional routes respectively)

4. Cloud Structures and the Evolution Features.

4.1 Evolution of Satellite Cloud Parameters

From before dawn to noon on September 19th, Drizzles appear in Liupan mountain area with the influence of precipitation clouds. Clouds propagate from Southwest to Northeast and the propagation velocity is about 40km•h^{-1}. It is seen from liquid water path retrieved by FY2 satellite that the cloud top height (at 5-7km) increases first and declines afterwards from 6: 00a.m. to 11: 00a.m. on September 18th. The cloud liquid content increases with the ascent of cloud top height. During this process, the ground precipitation is weak (about 1mm•h^{-1}).

4.2 Vertical Structures of Clouds

From sounding data at 08: 00 a.m. on September 19th in Yuzhong and Pinliang, the precipitation cloud is thick. The clouds in Yuzhong are 4 layers where the height of bottom cloud is 2413m, the height of top cloud is 11225m and the height of 0℃ layer is 4659m; The clouds in Pinliang are 3 layers where the height of bottom cloud is 1571m, the height of top cloud is 11301m and the height of 0℃ layer is 4885m; Both the wind in top and middle in these two stations are from southwest and the wind speed is 16-24m•s^{-1}.

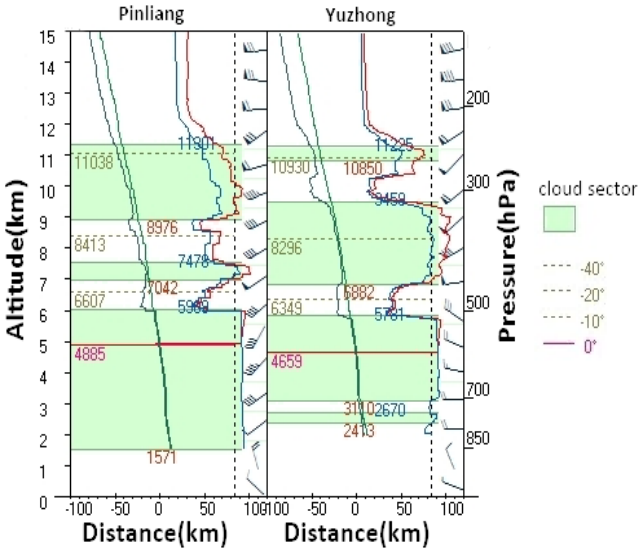

Figure 3: Cloud vertical structure diagram of Pingliang and Yuzhong sounding station on Setptember 19th

5. Cloud Precipitation Microphysical Structures

5.1 Diurnal Variations of Cloud and Precipitation Particle Distribution Features

Figure 4 to Figure 6 stand for the number concentration of 5~50μm cloud particles retrieved by BCP, cloud particles

retrieved by CIP and precipitation particles retrieved by PIP. It can be inferred that in the first stage (06: 26-07: 10), when the plane takes off, it climbs toward Jingyuan, both the cloud particle concentration and effective particle diameter increased in the uniform speed process, which indicates that the cloud turns thicker at southern place. There are larger fluctuations of cloud particle concentrations effective particle diameter in the climbing process indicating an unevenness horizontally. In the second and fifth stage (07: 10-07: 25, 08: 24-08: 32), the concentration of cloud particle detected by BCP is low while the effective particle diameter is comparatively larger.

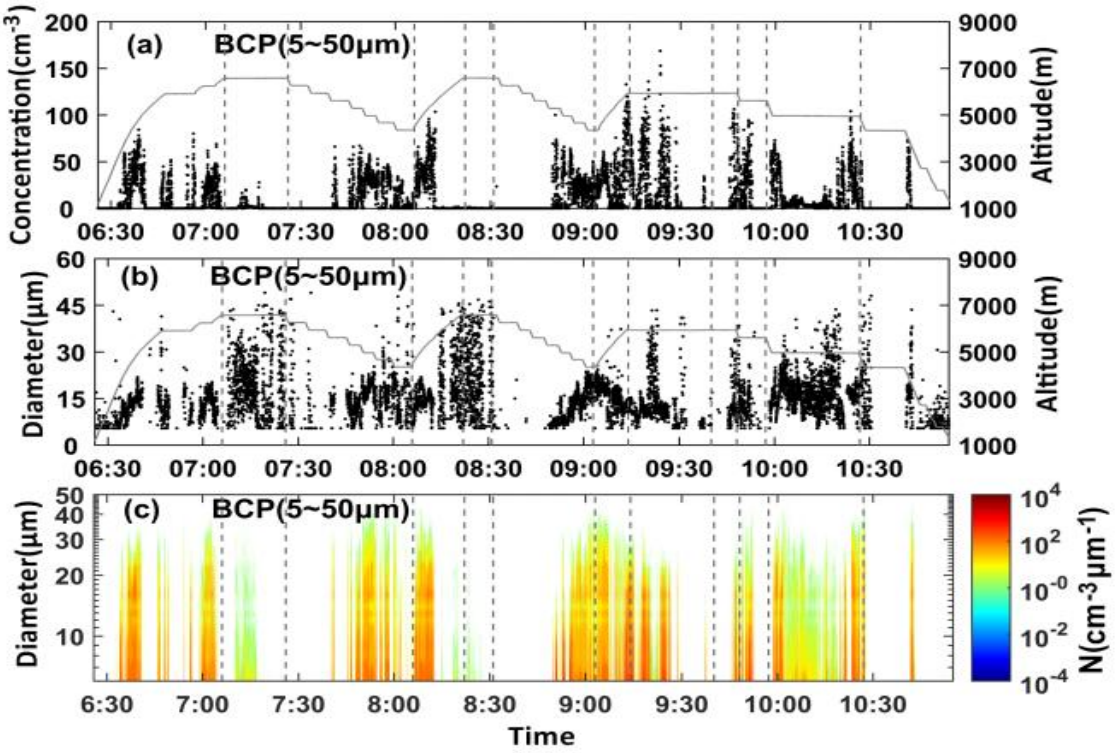

Figure 4: BCP (5~50μm) distributions with time (a: the number concentration, b: the effective particle diameter, c: the particle spectrum distribution).

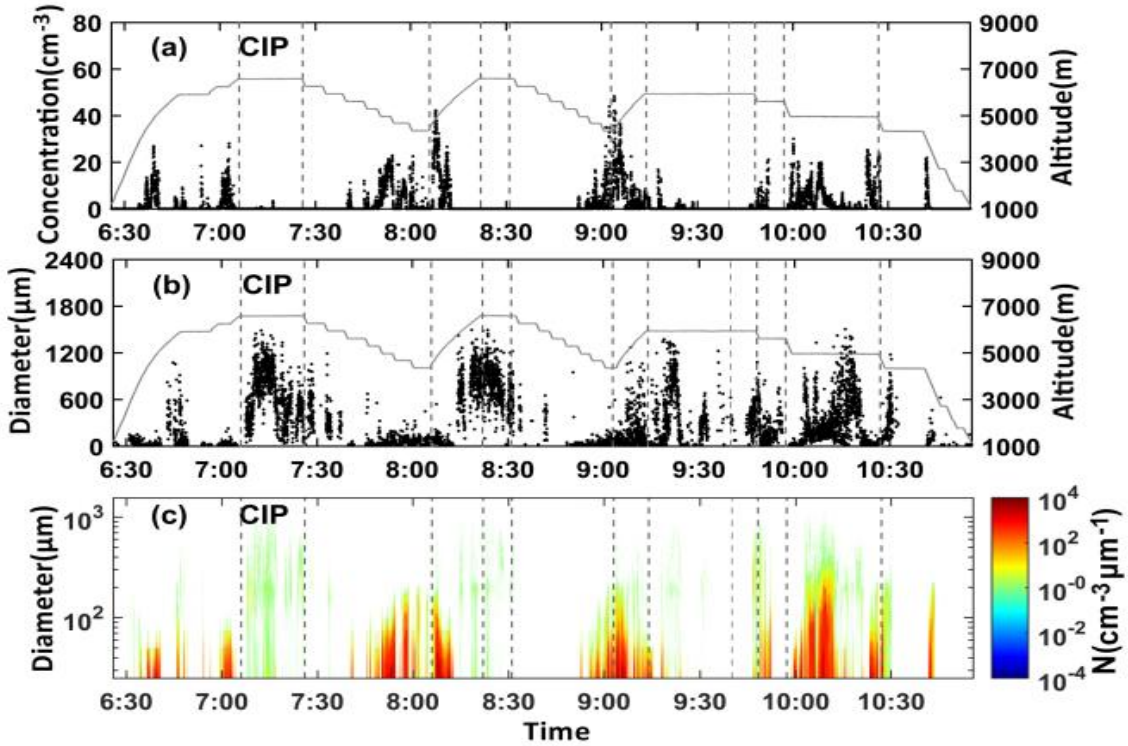

Figure 5: CIP distributions with time (a: the number concentration, b: the effective particle diameter, c: the particle spectrum distribution).

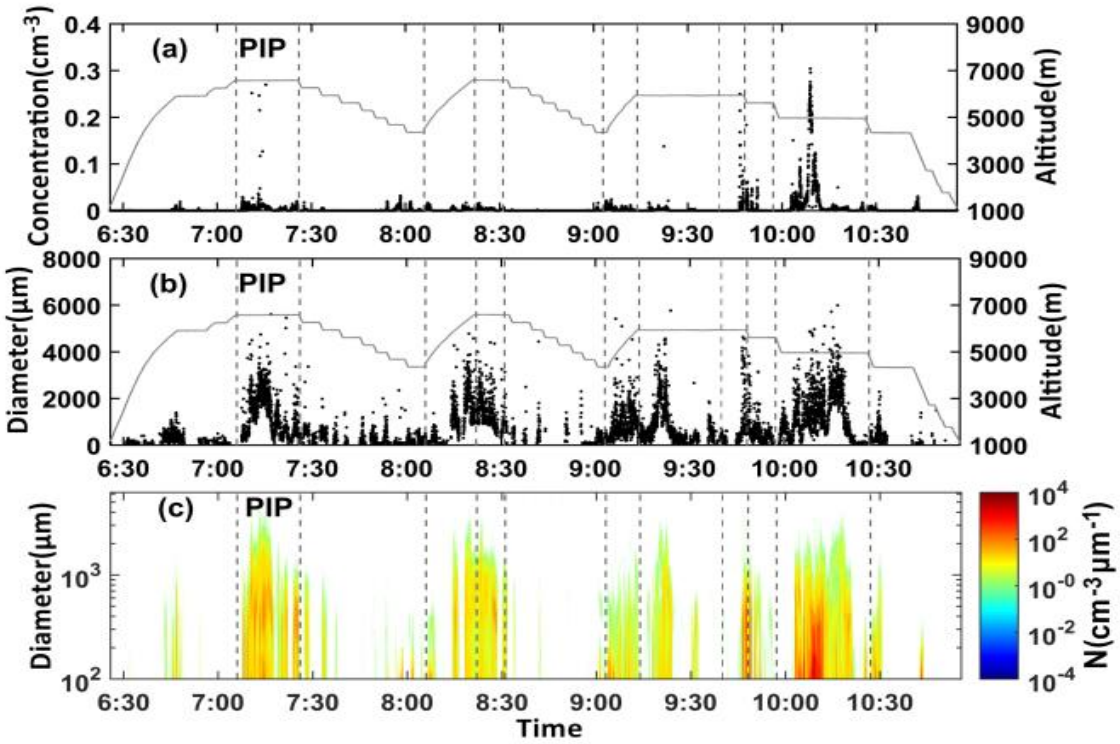

Figure 6: PIP distributions with time (a: the number concentration, b: the effective particle diameter, c: the particle spectrum distribution).

The spectrum of which is unimodal and the particle size less than 20μm is the majority. Larger particles detected by CIP as well as precipitation particle concentrations detected by PIP are small, while the effective particle diameter is comparatively larger. The spectrum of which is bimodal, there are another peaks at 200μm (CIP) and at 500μm (PIP). In this process, the temperature layer of level flight is around -8℃, where solid particles might be dominant. In the 3rd and 4th stage (07: 25-08: 07, 08: 07-08: 24) as well as the 6th and 7th stage (08: 32-09: 04, 09: 04-09: 15), In the process of vertical detection at West and East side of Liupan Mountain, small cloud particles detected by BCP as well as large particle concentrations detected by CIP are low while effective diameters are large above 5000m; small cloud particles detected by BCP as well as large particle concentrations and effective diameters detected by CIP are comparatively larger below 5000m. In the 8th stage (09: 15-09: 43), the plane is in level flight at 5940m, during which the trend of cloud particle concentrations is oppposite to that of the effective diameter. cloud particles detected by CIP are large in effecive diameter but low in number concentrations, and the width of spectrum is narrow. Likewise, the particle effective diameters detected by PIP are large but the number concentrations are low, during which weak precipitaion can be seen. In the 9th and 10th stage (09: 43-09: 47, 09: 47-09: 58), Cloud seeding is carried out repeatedly, cloud particle concentration (5-50μm) detected by BCP is lower than 20 cm^{-3} from 9: 43.Cloud particle concentration (5-50μm) detected by BCP is larger than 20 cm^{-3} with the maximum reaches 100 cm^{-3}.Meanwhile, when the large particle concentrations detected by CIP is less than 20 L^{-1}, it usually indicates a favorable seeding zone. the 11th stage (09: 58-10: 28) is level flight from Jinyuan to Huanxian at a height of 5100m (the mean temperature is -1.4℃), during which small cloud particles detected by BCP is large; The effective particle diameters and number concentrations of large particle concentrations detected by CIP are large, so are the sprectrum width; the effective particle diameters and number concentrations of large particle concentrations detected by PIP are large, during which precipitaion with large raindrops can be seen. In the 12th stage (10: 28-10: 54), the plane returns.

In the whole flight process, the Cloud particle concentrations (5-50μm) detected by BCP is 9.63 cm^{-3}, the number concentration is 168.78 cm^{-3}, which occurred during the flight from West side to East side of Liupan mountain at a hight of 5930m (the temperature is -5.6℃); The mean effective diameter is 15.84μm and the maximum effective diameter is 49μm. The correlation of vertical small cloud particle concentration and diameter is positive at West side while it is negative at East side. The mean particle concentration and maximum number concentration detected by CIP are 1.89 cm^{-3} and 48.27•cm^{-3} respectively, which occured during the flight from West side to East side of Liupan mountain at a hight of 5930m (the temperature is -5.6℃); The mean effective diameter is 160μm and the maximum effective diameter is 1507μm. Hobbs (1991) pointed out that regions where the concentration of cloud particles (≥2μm) is more than 10 cm^{-3} can be regarded as cloud water zone. Tao et al. (2001) proposed that a criterion for airplane cloud seeding: When the particle concentration detected by FSSP-100-ER detector is no less than 20 cm^{-3}, the cloud is seedable; when the particle concentration detected by 2DC detector is no less than 20 L^{-1}, the cloud is highly seedable. According to this criterion, half time of this flight is seedable at a height of 3000-5000m.

5.2 Vertical Probe at East and West Side of Liupan Mountains

In order to know the microphysical features of clouds at two sides of Liupan Mountain, vertical detection is carried out

from 7: 25a.m. at a height of 6600m near West side of Liupan Mountain. The plane made 4-km-radius circle detection every 300m descend, each time lasts 2-4 minutes until a height of 4300m, and then the plane ascends to 6600m in circles and the detection of West side is finished; The plane made 4-km-radius circle detection every 300m descend, each time lasts 2-4 minutes until a height of 4300m, and then the plane ascends to 6600m in circles and the detection of East side is finished. In the following part, downward vertical detection and upward vertical detection are discussed seperately.

5.2.1 Vertical detection of spiral rise

The verticle distribution of cloud particles and raindrops distribution during upward circling detection is shown in Figure 7. It can be inferred that there are extra layers in the cloud of West Liupan mountain and the detection height can be devides as 3 layers.

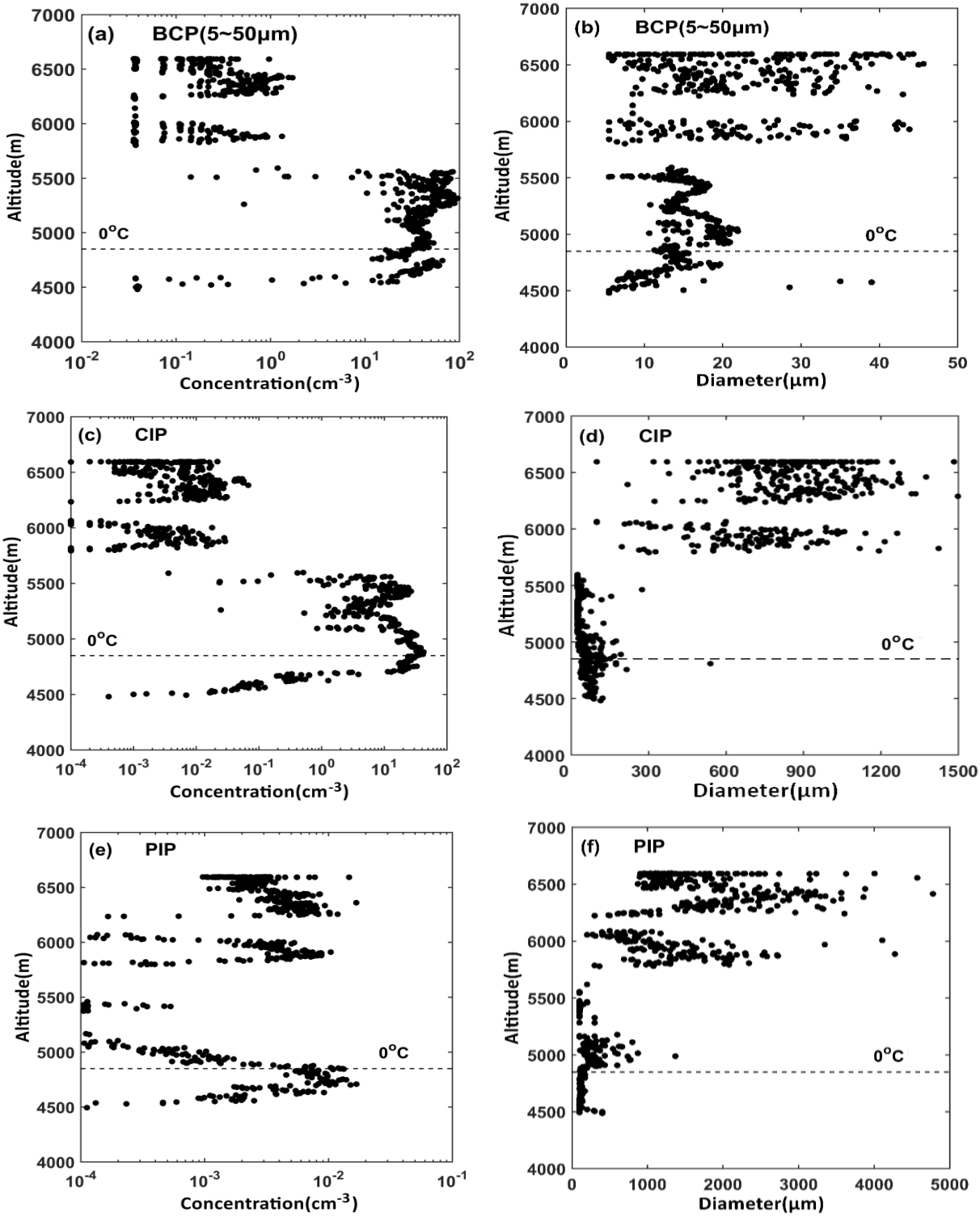

Figure 7: The vertical distribution of cloud and precipitation particles in the vertical detection stage on the west side of Liupan Mountain (a: the number concentration detected by BCP, b: the effective particle diameter detected by BCP, c: the number concentration detected by CIP, d: the effective particle diameter detected by CIP, e: the number concentration detected by PIP, f: the effective particle diameter detected by PIP)

In the first cloud layer, the cloud bottom is at 6250m (-5.5℃) and the cloud top is above 6600m (-8.2℃), the cloud thickness is larger than 350m; the variation of small cloud particles detected by BCP and large particle number concentrations detected by CIP with height is negligible, the number concentrations varies in a range of 0.05~1.1cm^{-3} and 3×10^{-3}~10^{-1}cm^{-3}, and the effective diameters varies in a range of 5~45μm and 200~1400μm. The raindrop particle number concentration dectected by PIP increases as the height declines and varies in a range of 10^{-3}~10^{-2}cm^{-3}, the effective diameter increases at first and then decreases as the height declines and the diameter varies in a range of 1000~4000μm.As a whole, the hydrometeror concentration of this cloud layer is low while the range of effective diameter is large from several microns to thousand microns. Since the concentration detected by BCP showed there are little super cooled water, in that case, the particle in cloud is mostly likely to be ice, grauple and snowflakes.

In the second cloud layer, the cloud bottom is at 5800m (-3.5℃) and the cloud top is above 6050m (-4.8℃), the cloud thickness is larger than 250m; the variation of small cloud particles detected by BCP and large particle number concentrations detected by CIP increases as the height declines and varies in a range of 0.05~1.1 cm^{-3} and 10^{-3}~10^{-1} cm^{-3}, the effective diameter increases at first and then decreases as the height declines and the diameter varies in a range of 5~45μm and 200~1200μm, the number concentrations varies in a range of 0.05~1.1cm^{-3} and 3×10^{-3}~10^{-1}cm^{-3}, and the effective diameters varies in a range of 5~45μm and 200~1400μm. The raindrop particle number concentration dectected by PIP increases first and then decreases as the height declines and varies in a range of 10^{-4}~10^{-2}cm^{-3}, the effective diameter increases at first and then decreases as the height declines and the diameter varies in a range of 600~2800μm. Since the cloud is thin, the relative humidity inside cloud is 72% ~82% and increases first and then decreases as the height declines, which indicate Dry air intrusion from the boundary of cloud, leading to a lower relative humidity at the edge of cloud. The closer to the edge, the stronger the evaporation, resulting a smaller number concentration and e effective diameter. There are little super cooled water, in that case, the particle in cloud is mostly likely to be ice, grauple and snowflakes.

In the third cloud layer, the cloud bottom is at below 4300m (1.5℃) and the cloud top is 5500m (-3.2℃), the cloud thickness is larger than 1200m; the variation of small cloud particle number concentrarion and effective diameter detected by BCP is similar, both of which increase at first and then decrease and again increase and decrease as the height declines. the number concentration is 100 times higher than the first and second cloud layers and vary in a range of 10~100cm^{-3}, and the effective diameter is less than that in the first and second cloud layers and vary in a range of 5~23μm. The variation of small cloud particle number concentration detected by BCP and that of large cloud particle number concentration detected by CIP with height is similar, which vary in a range of 1~80cm^{-3}; the effective diameter increases as the height declines and varies in a range of 100~220μm. Above 5100m, the raindrop particle number concentration and effective diameter dectected by PIP are small, which is less than 10^{-3} cm^{-3} and less than 500μm respectively. While the raindrop particle number concentration increases significantly as the height declines which vary in a range of 10^{-4}~2×10^{-2}cm^{-3}, the effective diameter varies in a range of 100~1400μm.Since the concentration detected by BCP showed is larger than 10cm^{-3}, supercooled water should exist in all cloud layers. From 300m below 0℃ temperature layer to 0℃ temperature layer, large cloud particles and raindrops increase and grow up, indicating an obvious Bergeron mechenism, Below the 0℃ temperature layer (at a height of 4850m), The small cloud particle number concentration detected by BCP decreases as the height declines, while at a height of 4700m, the number concentration increases significantly from 10 cm^{-3} to 80 cm^{-3}; the effective diameter increases at first and then decreases as the height declines and the variation ranges are similar to those above 0℃ temperature layer. Large cloud particle number concentration detected by CIP decreases as the height declines while the effective diameter increases as the height declines and the variation ranges are similar to those above 0℃ temperature layer. The raindrop particle number concentration dectected by PIP increases first and then decreases as the height declines and varies, the variation of effective diameter with height is not obvious.

The spectrum of cloud particles and raindrops distribution during circling detection along East of Liupan mountain is shown in figure 8. It is seen that there are no interlayer inside clouds and only one layer at detection height.

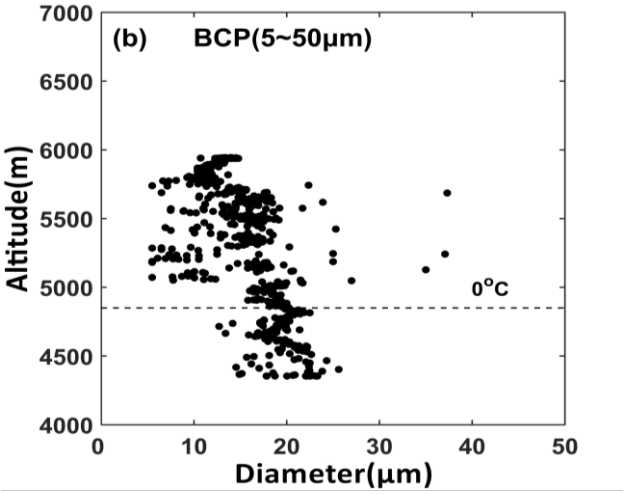

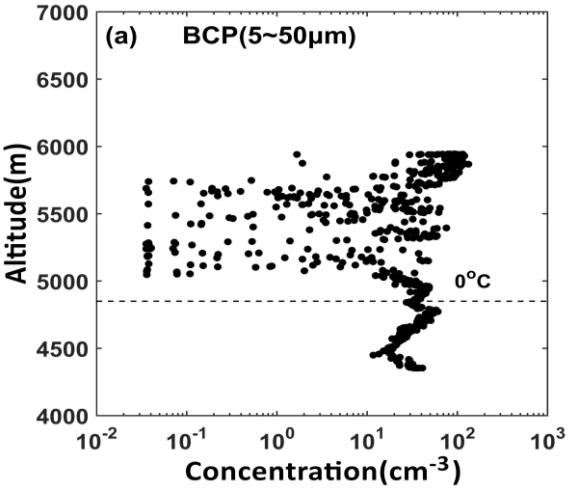

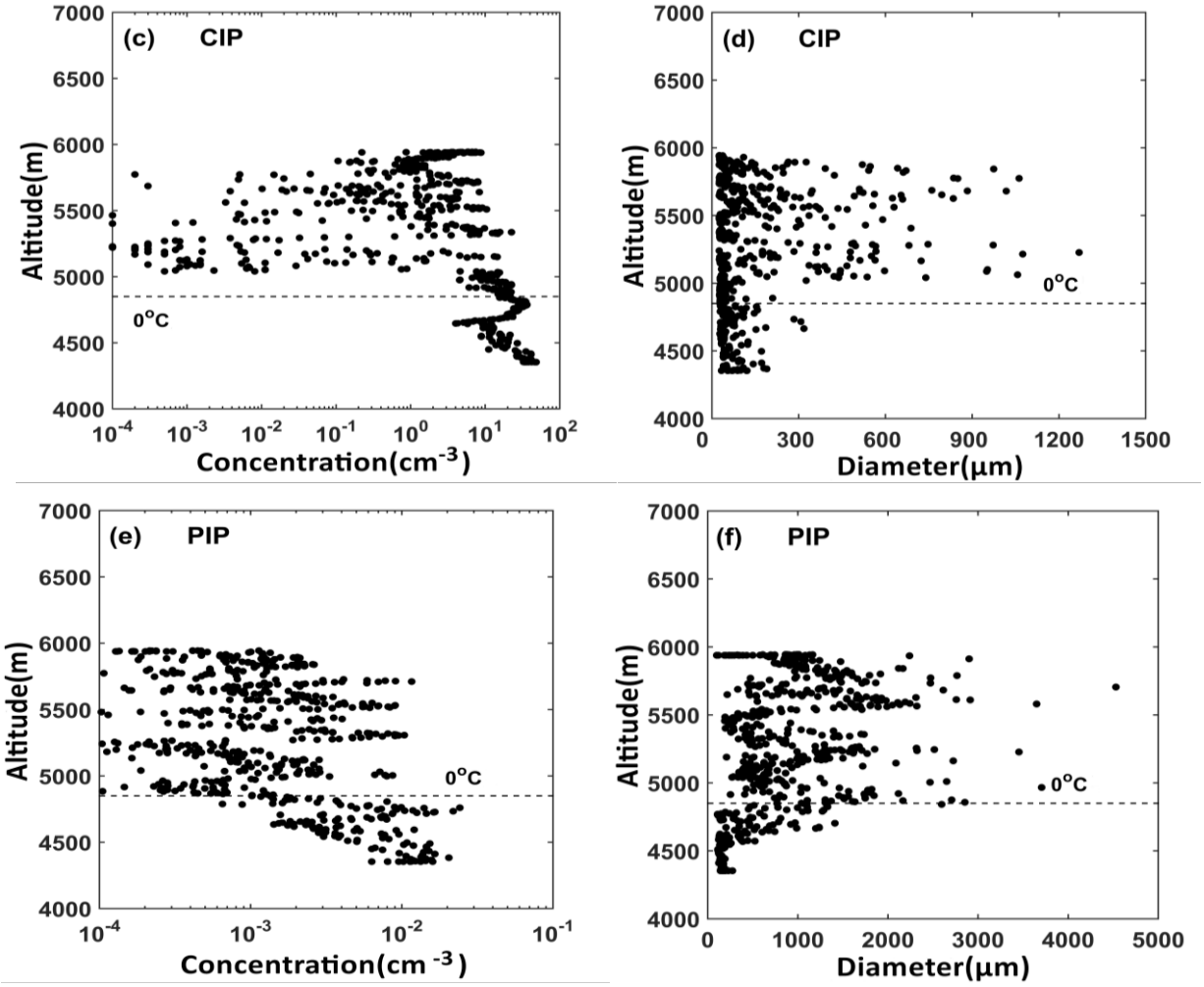

Figure 8: The vertical distribution of cloud and precipitation particles in the vertical detection stage on the east side of Liupan Mountain (a: the number concentration detected by BCP, b: the effective particle diameter detected by BCP, c: the number concentration detected by CIP, d: the effective particle diameter detected by CIP, e: the number concentration detected by PIP, f: the effective particle diameter detected by PIP)

Below the 1.6℃ temperature layer (at a height of 4300m), the cloud top is 5940m (-4.8℃), the cloud thickness is larger than 1640m; The small cloud particle number concentration detected by BCP decreases as the height declines; the effective diameter increases as the height declines and the variation ranges are similar to those above 0℃ temperature layer. The number concentration is similar to that of the West side of Liupan mountains but the variation range is larger in 0.05~100cm^{-3}; the effective diameter is similar to that of West side except more large cloud drops exist. Large cloud particle number concentration detected by CIP increases as the height declines, the number concentration is less than that of the West side of Liupan mountains in a range of 10^{-4}~50 cm^{-3}; the effective diameter ranges in 100~1300μm and large cloud drops exist. The raindrop particle number concentration and effective diameter are highly fluctuated as the height declines, which ranges in 10^{-4}~1×10^{-2}cm^{-3} and 100~4600μm. Since the concentration detected by BCP showed is larger than 10cm-3, supercooled water should exist in all cloud layers, however, the growth of cloud particles and raindrops are not obvious.

Below the 0℃ temperature layer (at a height of 4850m), The small cloud particle number concentration and effective diameter detected by BCP increase at first and then decrease and increase again as the height declines, the cloud particle number concentration ranges in 10~50•cm^{-3}; the effective diameter ranges in 12~28μm. Large cloud particle number concentration and effective diameter etected by CIP decreases as the height declines, the cloud particle number concentration ranges in 3~70•cm^{-3}; the effective diameter ranges in 50~350μm. The raindrop particle number concentration dectected by PIP increases first, then decreases and increases again as the height declines and varies, the effective diameter decreases as the height declines.

5.2.2 Downward stratified spiral vertical detection

The spectrum of cloud particles and raindrops distribution during circling detection along East and West side of Liupan mountain is shown in figure 9. The spectrum in two layers of cold clouds at three heights along West side is drawn with dot line, the spectrum below two layers of cold clouds and above 0℃ temperature layer at three heights along West side is drawn with solid line, the spectrum 0℃ temperature layer at two heights along West side is drawn with dashed line. The line types along East side are the same as West side.

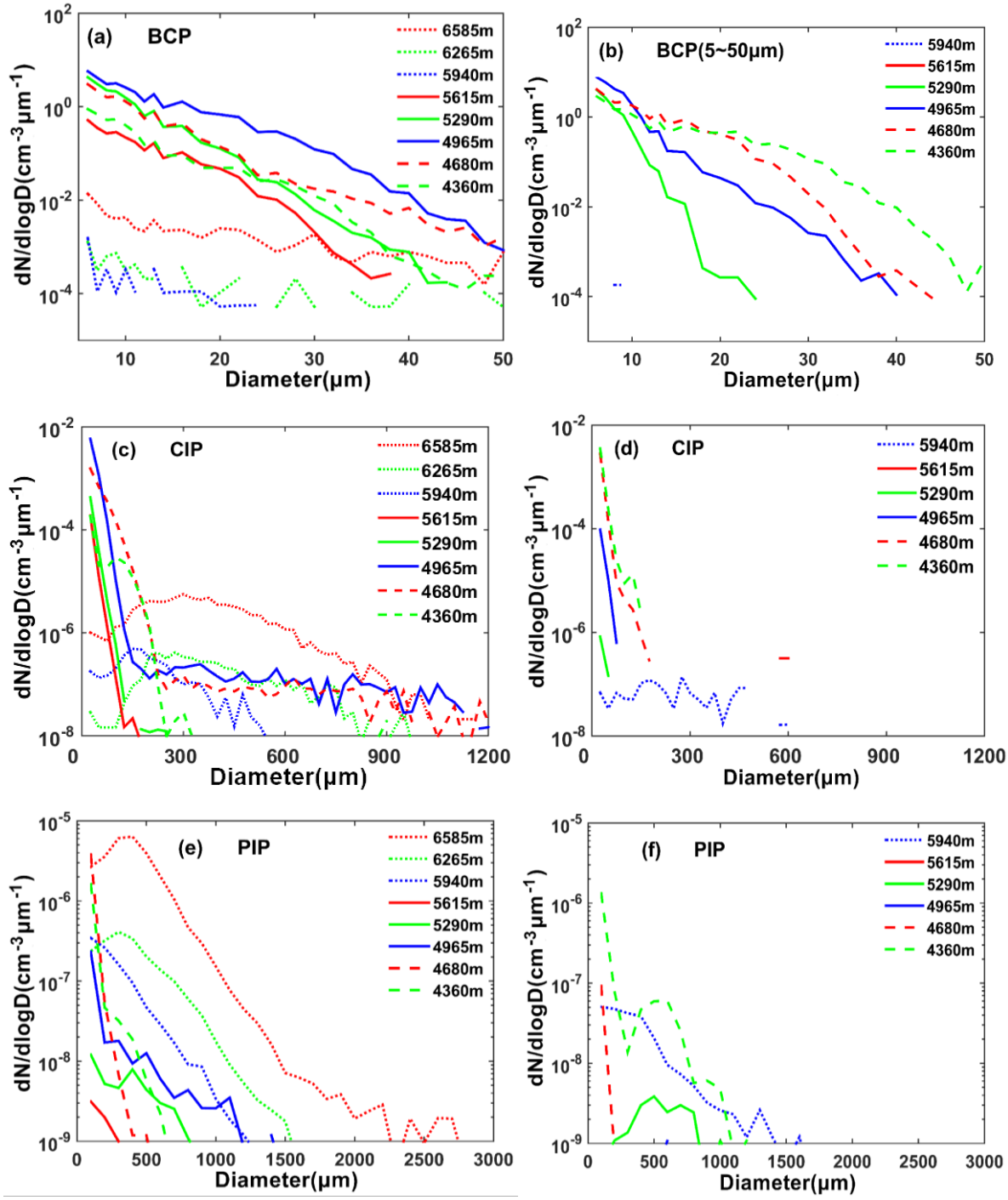

Figure 9: The particle spectrum distribution of stratiform precipitation at different heights in the east and west of Liupan Mountain

In Figure 9, as the height of two layers of cold clouds along West side declines, the spectrum width of small and big cloud particle as well as raindrop become narrower, the number concentration decreases. The distribution of small cloud particle spectrum is linear, the distribution of small cloud particle spectrum is linear, the distribution of big cloud particle and raindrops spectrum is unimodal, indicating a lower temperature is advantigeous for genesis of ice and snow.

When the mixed clouds below cold clouds are above 0℃ temperature layer, as the height declines, the spectrum width of small and big cloud particle as well as raindrop become wider, the number concentration increases. The distribution of small cloud particle spectrum is linear, the distribution of small cloud particle spectrum is linear, indicating the mutiplying of cloud particles and raindrops when they fall through cold cloud zone. When the mixed clouds are below 0℃ temperature layer, as the height declines, the spectrum width of small cloud particle stay same, but the number concentration decreases dramatically. As a whole, solid precipitation particles melt after falling through 0℃ temperature layer. The number concentrations of cloud particles in all sizes decrease to some extent, meanwhile, big cloud particles disappear due to melting.

Along East side of Liupan mountain, as the height declines, the spectrum width of small and big cloud particle as well as

raindrop become wider, the number concentration increases, which is the same as West side. When the mixed clouds are below 0℃ temperature layer, as the height declines, the number concentration especially that of big drops increase dramatically, which could be attributed to a strengthened coalescence growth of droplets below 0℃ temperature layer.

5.3 Analysis of Cloud Seeding Effect

The cloud seeding operation is carried out in a "Z" route at a height of 5940m (the temperature layer is -6℃~-5.2℃) from 09: 15a.m. to 09: 42a.m..The seeding frame got frozen, indicating the abundance of supercooled water. Four silver iodide flare sticks are used in this process, each of them weighs 2.5 kg and contains 125g silver iodide, the nucleation rate is about 10^{14} min^{-1} at -10℃. Round trip detection is is carried out a height of 5940m and 5615m, the cloud microphysical parameters are listed as Table 3.

Table 1: Changes of cloud microphysical parameters before and after seeding

	N_{BCP} (/cm^3)	D_{BCP} (um)	N_{CIP} (/cm^3)	D_{CIP} (um)	N_{PIP} (/cm^3)	D_{BCP} (um)
before seeding (6000m)	29	16	0.66	329	1.3×10^{-3}	793
after seeding (6000m)	14	9	5×10^{-3}	238	2×10^{-5}	256
after seeding (5600m)	43	16	1.43	275	4.44×10^{-2}	752

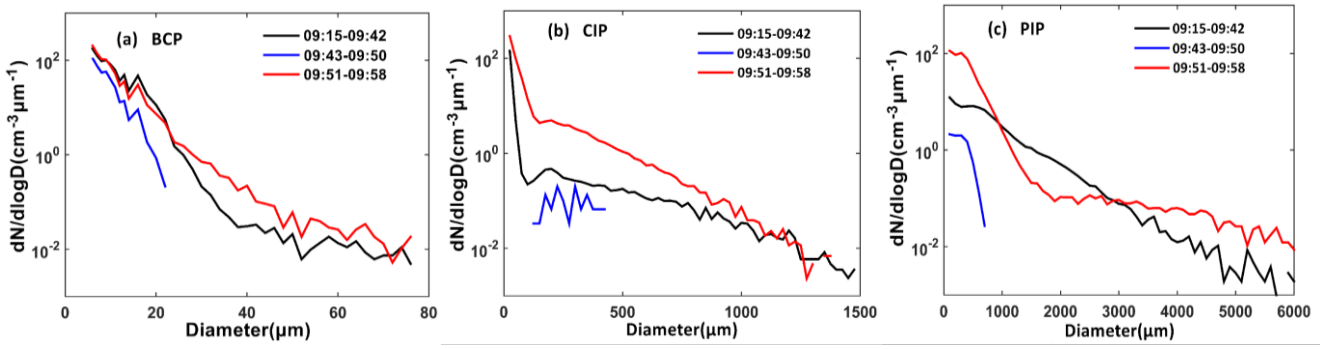

Figure 10: The variation of cloud and precipitation particle spectrum before and after seeding

In figure 10, the spectrum width of cloud particles and raindrops get narrower significantly at the same height, while the number concentration of cloud particles and raindrops increase a lot at 400m below that height. Particles with a diameter less than 1000μm increase, those between 1000-3000μm decrease, and those above 3000μm increase. The results indicate the change of cloud particles and raindrops are not obvious, however, the number concentration of cloud particles and raindrops increase a lot at 400m below that height and the spectrum width is broadened, which is advantageous for cloud growth and increase of surface precipitation.

6. Summary and Discussions

The rainfall process is under the joint influence of cold air mass and warm and moisture airflow outside the subtropical high,. There are two ridges-one trough, and a low pressure during which the rain band moves from South to North at a speed of 40km•h^{-1}., weak rainfall appear in Liupan mountain area, the rain rate is about 1mm•h^{-1}.

During flight detection period, the mean number concentration of 5~50μm cloud particles detected by BCP is about 9.63 cm^{-3}, mean number concentration detected by CIP is about 1.89 cm^{-3}, and mean effective diameter is about 160μm;the maximum number concentration of 5~50μm cloud particles detected by BCP is about 168.78 cm^{-3}, detected by CIP is about 48.27 cm^{-3}, which occurred during the flight process from West side to East side of Liupan mountain at a height of 5930m (-5.6℃ temperature layer).half time of this flight is seedable at a height of 3000-5000m.

There are two layers of clouds along West side of Liupan mountain, the clouds at top layer are thin, the cloud particles of which are mainly ice, grauple and snow. The clouds at bottom layer are mixed clouds. In the colder layer of mixed clouds, there exists supercooled water, as the height declines, the spectrum of small and big cloud particles as well as raindrops become wider, and the number concentrations become larger; In the warmer layer of mixed clouds, as the height declines, the spectrum of small cloud particles stay the same but the number concentrations decrease a great deal. Solid precipitation particles melt after falling through 0℃ temperature laye,, the number concentration especially that of big drops increase dramatically due to a strengthened coalescence growth of droplets, meanwhile, big cloud particles disappear because of melting.

There is one layer of mixed cloud along East side of Liupan mountain. In the colder layer of mixed cloud, as the height declines, the spectrum of small and big cloud particles as well as raindrops become wider, and the number concentrations become larger, which is the same as West side; In the warmer layer of mixed clouds, as the height declines, the number concentration especially that of big drops increase dramatically, which could be attributed to a strengthened coalescence growth of droplets below 0℃ temperature layer.

The correlation between number concentration and diameter in vertical direction is positive along West side of Liupan mountain, while that of East side is negative. he change of cloud particles and raindrops are not obvious, however, the number concentration of cloud particles and raindrops increase a lot at 400m below that height and the spectrum width is broadened.

Author Contributions

Conceptualization, Z.C. and L.T.; methodology, L.T.; software, L.T.; validation, L.T. and T.L.; formal analysis, L.T.; investigation, N.C.; resources, Z.C.; data curation, T.L.; writing—original draft preparation, T.L. and Y.S.; writing—review and editing, Z.C.; visualization, Y.S.; supervision, Z.C.; project administration, Z.C. and L.T.; funding acquisition, Z.C., L.T. and H.Z. All authors have read and agreed to the published version of the manuscript.

Funding:

This research was funded by The Natural Science Foundation of Ningxia (2023AAC03800) and National Natural Science Foundation of China (U22A20577).

References

[1] Dang Juan, Wang Guanghe, Liu Weiguo, et al. A case analysis on microphysical characteristics of summer stratiform cloud in Gansu province[J]. Meteorological Monthly, 2009, 35 (1): 24-36. (in Chinese).

[2] Dong X, Zhao C, Yang Y, et al.Distinct change of supercooled liquid cloud properties by aerosols from an aircraft-based seeding experiment. Earth and Space Science, 2020, 7, 1-11.doi: 10.1029/2020EA001196.

[3] Houze R A, Hobbs P V, Herzegh P H, et al. Size distribu-tions of precipitation particles in frontal clouds [J]. J Atmos Sci, 1979, 36: 156-162.

[4] Hobbs P V, Matejka T J, Herzegh P H, et al. The mesoscale and microscale structure and organization of clouds and precipitation in midlatitude cyclones. I: A case study of a cold front[J]. J. Atmos. Sci., 1980, 37: 568-596.

[5] Hobbs P V, Rangno A L. Ice particale concentrations in clouds [J]. J. Atmos. Sci., 1985, 23: 2523-2549.

[6] Hobbs P V. Twenty Years of Airborne Research at the University of Washington[J]. Bulletin of the American Meteorological Society, 1991, 72 (11): 1707-1717.

[7] Huang Mengyu, Zhao Chunsheng, Zhuo Guangqiang, et al. Stratus cloud microphysical characters over north China region and the relationship between aerosols and clouds [J]. Journal of Nanjing Institute of Meteorology, 2005, 28 (3): 360–368. (in Chinese).

[8] Huang Meiyuan. Cloud and precipitation physics [M]. Beijing: Science Press, 1999. (in Chinese).

[9] Hou Tuanjie, Hu Zhaoxia, Lei Hengchi. A study of the structure and microphysical processes of a precipitating stratiform cloud in Jilin[J]. Acta Meteorologica Sinica, 2011, 69 (3): 508–520. (in Chinese).

[10] Hong Yanchao, Li Hongyu. Cloud structure, precipitation mechanism, and artificial enhancement precipitation condition for a frontal stratiform cloud system [J]. Plateau Meteorology, 2011, 50 (3): 1308–1323. (in Chinese).

[11] Fan Shuxian. A case study on the evolution of microphysical structure of stratiform cloud[J]. Journal of Ningxia University (Natural Science Edition), 2000, 21 (2): 180-182. (in Chinese).

[12] Fu, Y., H. Li, and Y. Zi. Case Study of Precipitation Cloud Structure Viewed by TRMM Satellite in a Valley of the Tibetan Plateau[J]. Plateau Meteorology, 2007, 26, 98-106.

[13] Feng Qiujuan, Li Peiren, Ding Jian-fang, et al. Observation and analysis of microphysical characteristics of stratiform cloud precipitation in Shanxi Province[J]. Trans Atmos Sci, 2013. 36 (5): 537-545. (in Chinese).

[14] Fu, Y., and G. Liu. Possible Misidentification of Rain Type by TRMM PR over Tibetan Plateau[J]. Journal of Applied Meteorology and Climatology, 2017, 46, 667-672.

[15] Li J, Li P, Ren G, et al. Aircraft measurements of aerosol distribution, warm cloud microphysical properties, and their relationship over the Eastern Loess Plateau in China[J]. Tellus B: Chemical and Physical Meteorology, 2019, 71 (1): 1-17. doi: 10.1080/16000889. 2019. 1663994

[16] Ma Xincheng, Huang Mengyu, Yu Xiaowei, et al. An observational study of macro/microphysical structures of stratiform cloud in a high-pressure system rear over mountain [J]. Climatic and Environmental Research (in Chinese), 2012, 17 (6): 711–718. (in Chinese).

[17] Pang Zhaoyun, Huang Shan, Zhang Fengwei. Microphysical structure of a stratiform cloud precipitation event in central Gansu province [J]. Meteorological Science and Technology, 2016, 44 (5): 805-810. (in Chinese).

[18] Qin Yanshuo, LIU Shixi, FAN Genchang, et al. Analysis on microphysical characteristics and seedability of a stratiform cloud in spring over north china [J]. Journal of Arid Meteorology, 2015, 33 (3): 481-489. (in Chinese).

[19] Qin Yanshuo, Cai Miao, Liu Shixi, et al. A study on macro and micro physical structures of convective - stratiform mixed clouds associated with a cold front in autumn and their catalytic responses in North China. Acta Meteorologica Sinica, 2017, 75 (5): 835-849. (in Chinese).

[20] Qi Peng, GUO Xueliang, LU Guangxian, et al. Aircraft Measurements of a Stable Stratiform Cloud with Embedded Convection in Eastern Taihang Mountain of North China: Characteristicsof Embedded Convection and Melting Layer Structure [J]. Chinese Journal of Atmospheric Sciences, 2019, 43 (6): 1365-1384. (in Chinese).

[21] Sun Yuwen, Li Baodong, Liu Wei, et al. Study on Physical Structure of Hebei Stratiform Clouds in Autumn and Its Seedability Condition

[22] [J]. Plateau Meteorology (in Chinese), 2015, 34 (1): 237-250. (in Chinese).

[23] Sun Yuwen, Dong Xiaobo Li Baodong, et al. The physical properties and seeding potential analysis of a low trough cold front cloud system at mountain Taihang based on Aircraft observations[J]. Plateau Meteorology (in Chinese), 2019, 38 (5): 971-982. (in Chinese).

[24] Tao S W, Liu W G, Hu Z J, et al. Technology research on the seedability of artificial precipitation on cold layer cloud [J].J Appl Meteor Sci, 2001, 12 (S): 14-22. (in Chinese).

[25] Wang Lijun, Yin Yan, Yao Zhanyu, et al. Microphysical responses as seen in a stratocumulus aircraft seeding experiment in autumn over the Sanjiangyuan nature reserve [J]. Acta Meteorologica Sinica, 2013, 71 (5): 925-939. (in Chinese).

[26] Wang Lijun, Yin Yan, Li Lunge, et al. Analyses on typical autumn multi–layer stratiform clouds over the Sanjiangyuan National Nature Reserve with airborne observations [J]. Chinese Journal of Atmospheric Sciences, 2013, 37 (5): 1038–1058. (in Chinese).
[27] Wang Yanfeng, HUANG Wubin, HE Cuiying, et al. Analysis on Microphysical Structure of Stratiform Clouds in Autumn in Loess Plateau of Middle Gansu[J]. Journal of Arid Meteorology, 2017, 35 (1): 64-72. (in Chinese).
[28] Wang Y, Niu S, Lu C, et al. An Observational Study on Cloud Spectral Width in North China[J]. Atmosphere, 2019, 10 (3): 109.doi: 10.3390/atmos10030109.
[29] Wang J, Yue Z, Daniel Rosenfeld, et al. The Evolution of an AgI Cloud-Seeding Track in Central China as Seen by a Combination of Radar, Satellite, and Disdrometer Observations[J]. Journal of Geophysical Research: Atmospheres, 2021, 126 (11): e2020JD033914 - e2020JD033914.doi: 10.1029/2020JD033914.
[30] Wei L, Huang M, Zhang R, et al. Microphysical characteristics of precipitating cumulus cloud based on airborne Ka-band cloud radar and droplet measurements [J]. Atmospheric and Oceanic Science Letters, 2021, 15: 1-6.doi: 10.1016/J.AOSL.2021.100134.
[31] Xiang Lei, Niu Shengjie. Anasis of the macro and micri physical characteristics of stratiform clouds in Ningxia [J]. Scientia Meteorologica Sinica, 2008, 28 (3): 258-263. (in Chinese).
[32] Yang Wenxia, NIU Shengjie, WEI Junguo, et al. Airborne Observation for Microphysical Structure of Precipitation System of Stratiform Cloud in Hebei Provice [J]. Plateau Meteorology, 2005, 24 (1): 84-90. (in Chinese).
[33] Zhang Dianguo, Yao Zhanyu, Gong Dianli, et al. Microphysical structures of stratocumulus mixed cloud detected by aircraft around Beijing area[J]. Trans Atmos Sci, 2011, 34 (1): 109-121. (in Chinese).
[34] Zhang Yu, Yin Yan, Shi Lixin, et al. Analysis of cloud microphysics structure over Hebei region during autumn of 2007[J]. Plateau Meteorology, 2012, 31 (2): 530-537. (in Chinese).
[35] Zhao C, Qiu Y, Dong X, et al. Negative aerosol-cloud re relationship from aircraft observations over Hebei, China[J]. Earth and Space Science, 2018, 5 (1): 19–29.doi: 10.1002/2017EA000346
[36] Zhao C, Zhao L, Dong X. A case study of stratus cloud properties using in situ aircraft observations over Huanghua, China [J]. Atmosphere, 2019, 10 (1): 19. doi: 10.3390/atmos10010019